Chabazite : stable cation-exchanger in hyper alkaline concrete pore water

Chabazite: Stable cation-exchanger in hyper alkaline concrete pore water

Leen Van Tendeloo,[1] *Wauter Wangermez,* [1] *Mert Kurttepeli,* [2] *Benny de Blochouse,* [1] *Sara Bals,* [2] *Gustaaf Van Tendeloo,* [2] *Johan A. Martens,* [1] *André Maes,* [1] *Christine E.A. Kirschhock,* [1] *Eric Breynaert*[1,]*.

[1]Centre for Surface Chemistry and Catalysis, KU Leuven, Kasteelpark Arenberg 23 – box 2461, 3001 Heverlee.

[2]Electron Microscopy for Materials Science (EMAT), University of Antwerp, Groenenborgerlaan 171, 2020 Antwerp;

cation exchange, cesium, zeolite stability, hyper alkaline media, chabazite, merlinoite, concrete porewater

ABSTRACT

To avoid impact on the environment, facilities for permanent disposal of hazardous waste adopt multi-barrier design schemes. As the primary barrier very often consists of cement-based materials, two distinct aspects are essential for the selection of a suitable complementary barriers: 1) selective sorption of the contaminants in the repository and 2) long-term chemical stability in hyperalkaline concrete derived media. A multidisciplinary approach combining experimental strategies from environmental chemistry and materials science is therefore essential

to provide a reliable assessment of potential candidate materials. Chabazite is typically synthesized in 1 M KOH solutions, but also crystallises in simulated young cement porewater, a pH 13 aqueous solution mainly containing K^+ and Na^+ cations. Its formation and stability in this medium was evaluated as function of temperature (60 and 85°C) over a timeframe of more than 2 years and was also asessed from a mechanistic point of view. Chabazite demonstrates excellent cation exchange properties in simulated young cement porewater. Comparison of its Cs^+ cation exchange properties at pH 8 and pH 13 unexpectedly demonstrated an increase of the K_D with increasing pH. The combined results identify chabazite as a valid candidate for inclusion in engineered barriers for concrete based waste disposal.

INTRODUCTION

Despite all efforts towards selective waste collection and consequent recycling, non-reusable and hazardous waste fractions remaining at the end of the revalorization chain, require long-term storage or permanent disposal.[1, 2] One example is the low- and medium-level, short-lived conditioned radioactive waste (in a Belgian context, category A waste),[3] which has to be stored safely for several decades up to centuries. As for chemotoxic waste, a feasible scenario for this waste involves immobilization and isolation in concrete-based surface disposal facilities.[1-6] The concrete acts as the main barrier in preventing the radionuclides from entering the biosphere. In order to increase the robustness of a disposal system complementary barriers can be implemented. Such a complementary barrier should combine long term stability in hyper-alkaline aqueous media with suitable sorption properties (high selectivity and excess capacity). Indeed, upon water intrusion and consequent rehydration of the concrete, the first cement degradation stage generates hyper-alkaline, saline pore water (0.1 - 1 M OH^-, 0.1 - 1 M alkaline cations) due to dissolution of Na_2O and K_2O (See Table SI- 1 for typical composition).[7, 8]

Prefereably, the sorption sink should be unsuitable as substrate for bacteria proliferation. In view of all these limitations, zeolites are among the few commercially available materials remaining on the shortlist of potentially suitable sorption sinks.

While the structure of a zeolite framework can be probed with several physicochemical characterization techniques such as XRD and NMR, chemical probes can be assumed to be more sensitive to detect zeolite hydrolysis, small changes in framework composition, and/or aluminium distribution. Since the affinity of an ion exchanger for specific ions (e.g. Cs^+ vs Na^+) is highly dependent on the surface charge density,[9-12] specific ions can be exploited as a probe for the site selectivity and hence charge distribution of a cation exchanger. Cs^+ has been adopted as a proxy to assess the potential use of zeolites in complementary barriers because it is a well-known species in neutral conditions exhibiting high sorption on zeolites.[13-23] While zeolite types such as CHA, HEU and MOR are known to selectively retain Cs^+ cations through ion-exchange, reports on their application and stability in hyper-alkaline aqueous media are scarce [18, 24, 25]. However, CHA is among the few framework types that have been reported to form upon interaction of young concrete pore water (YCW) with natural aluminosilicates. Equilibrating bentonite with simulated concrete pore water for a period of 2 years, Fernandez *et al.* observed the formation of chabazite at both 60 and 90 °C, and merlinoite at 90°C.[26] Also by reacting sediments containing chlorite as the dominant clay mineral with YCW for 1 year at 70°C, chabazite was formed.[27] Within the timeframe of these studies, no zeolite formation was detected at room temperature.

Next to these studies of zeolite formation upon sediment interaction with YCW, interaction of zeolites with inorganic hyper-alkaline aqueous media is also investigated and exploited for zeolite production. Indeed, hyper-alkaline transformation of synthetic zeolites based on

solubilization, followed by nucleation and growth of a new phase, is actively explored as a means to easily synthesize various zeolite types using cheap zeolitic starting materials (e.g. FAU).[28-30] In addition to easy access to industrially important frameworks, these experiments also allow extrapolation on the stability of zeolite frameworks in high alkaline conditions: The understanding of hyperalkaline transformation of zeolites, subsequently yielding stable phases in a specific medium, could add confidence towards long-term safety of zeolites as sorption sinks. This approach demonstrating the affinity for a specific framework to form and to be stabilized in high alkaline conditions, offers added value to the mere observation that this zeolite remains unaltered by short term exposure to YCW.

Estimation of zeolite stability in hyper-alkaline solutions (e.g. concrete pore water) over a timeframe of tens of decades, ultimately requires elucidation of the mechanism responsible for the (de)stabilizing effects of alkaline cations on zeolite structures. Therefore, this study aimed at enhancing insight into zeolite transformation processes and revealing the role of alkali metal cations therein. To increase confidence in the results, the zeolite transformation study in multiple Na/K based hyper-alkaline media as function of temperature, was combined with a chemical assessment of the stability of the main transformation product, chabazite, via time-dependent evaluation of its affinity for Cs^+ exchange.

EXPERIMENTAL SECTION

Materials. A commercial zeolite Na-Y (Zeocat, Si/Al =2.65) was used as starting material for the transformation study in concrete pore water. In addition, micron sized zeolite Y crystals were synthesized according to a recipe from Feijen *et al*. [31] using a batch composition 10 SiO_2: Al_2O_3: 2.40 Na_2O: 1 15-crown-5: 135 H_2O. To remove the 15-crown-5 template, the zeolite

87 powder was calcined in air for 10 hours at 550°C, with a heating rate of 2°C/min. The Si/Al ratio
88 of the calcined Na-Y was determined as 3.50 by ^{29}Si MAS NMR.
89 Chabazite for the sorption experiment was synthesized by hydrothermal transformation of
90 zeolite Y (Zeocat) according to the IZA recipe, [32] originally reported by Bourgogne *et al.*[33]
91 Ca-Y was obtained by ion-exchange of calcined (NH_4, Na)-Y (CBV300, Zeolyst) with 1 M
92 $CaCl_2$.
93 **Transformation study**. For the transformations in YCW, zeolite Na-Y (Zeocat, Si/Al = 2.65)
94 was used. All batch systems consisted of 40 mL Oak Ridge polypropylene (PP) centrifuge tubes
95 with screw caps containing 500 mg of zeolite Na-Y powder, sieved between 100 and 200 μm.
96 Upon addition of 20 mL of simulated YCW, the gross weight of the batch systems was logged
97 for future reference. One series of 20 tubes was placed in a rotary oven at 85°C, while a second
98 series was incubated statically at 60°C. To correct the liquid volume lost due to water vapour
99 diffusion through the PP tube, the tubes were topped up with milliQ water on a weekly basis for
100 the tubes incubated at 85°C and on monthly basis in the case of the series incubated at 60°C. The
101 chemical equilibria in the systems were evaluated as function of time by sacrificial analysis of
102 the components of one batch system for each evaluation time. At each evaluation time, one
103 system was cooled to room temperature, centrifuged and decanted. The pH of the supernatant
104 was measured and the pellet was dried overnight at 60°C.
105 Na-Y(Si/Al = 3.5) was immersed in 1.2 M KOH (VWR, min. 85%). All batch systems of this
106 series consisted of centrifuge tubes with screw caps containing 300 mg of Na-Y and 18 mL of
107 hydroxide solution. The PP tubes were placed in a rotary oven at 85°C. At each evaluation time,
108 one system was cooled to room temperature, centrifuged and decanted. The liquid was

immediately diluted 50 and 500 times with milliQ water. The solids were washed with water and dried at 60°C before characterization.

Ca-Y was exposed to 1 M KOH at 95°C, using a liquid/solid ratio of 9.

YCW. Simulated state I concrete pore water (pH 13) was obtained by mixing 500 mL Milli-Q water, 0.0296 g $Ca(OH)_2$ ($4 \cdot 10^{-4}$ mol), 10 mL Na_2CO_3 solution (10^{-2} M), 180 mL KOH (1 M), 70 mL NaOH solution (1 M), and 0.189 g $CaSO_4.2\ H_2O$ ($1.1 \cdot 10^{-3}$ mol) in this order. Upon complete dissolution of all components, the solution was made up to 1 L with Milli-Q water.

A moderate pH counterpart of the state I concrete pore water (pH 8) was prepared in a 1 L volumetric flask by dissolving respectively 0.189 g of $CaSO_4.2\ H_2O$ [1.1×10^{-3} moles] and 0.0945 g of $Ca(NO_3)_2.4\ H_2O$ in 500 mL of MilliQ water, followed by addition of 10 mL of a 10^{-2} M $NaHCO_3$ solution, 180 mL of a 1M KNO_3 solution, 70 mL of a 1M $NaNO_3$ solution. After complete dissolution of all components the total volume was made up to 1 L by addition of MilliQ water, immediately followed by a transfer of the solution to a closed 1 L polypropylene bottle.

Equilibrium speciation for the major elements was calculated with Phreeqc [34], in combination with the Lawrence Livermore National Laboratory database llnl.dat.

Characterization. The evolution of the solids was evaluated by XRD analysis. High resolution XRD patterns were recorded on a STOE STADI MP diffractometer with focusing Ge(111) monochromator ($CuK\alpha_1$ radiation) in Debye-Scherrer geometry with a linear position sensitive detector (PSD) (6 2°θ window) with a step width of 0.5 degree and internal PSD resolution 0.01 degree. High throughput PXRD screening was performed on a STOE STADI P Combi diffractometer with focusing Ge(111) monochromator ($CuK\alpha_1$ radiation) in transmission

geometry with 140°-curved image plate position sensitive detector (IP PSD) from with internal IP PSD resolution of 0.03 degree.

ICP-AES was used to determine Si and Al in supernatant solutions.

Scanning electron microscopy (SEM) was performed using a FEI Helios NanoLab 650 dual-beam system to resolve the morphology of the zeolitic crystals during the transformation in pure KOH. The products formed in YCW were studied using a FEI-Nova Nano-SEM 450. Transmission electron microscopy (TEM) specimens were prepared by applying drops of ethanol suspension of the powder sample on a carbon coated copper grid. High-resolution TEM (HRTEM) was performed using a FEI Tecnai F20 operated at 200 kV.

Tilt series for electron tomography were acquired with the FEI Tecnai F20 operated at 200 kV in combination with an advanced tomography holder from Fischione Instruments and the FEI XPlore3D acquisition software. Tilt series consisting of 75 HAADF-STEM images were acquired with tilt increments of 2° over a range of ±74° on TEM samples. Alignment of the data was carried out using the FEI Inspect3D software package. The reconstruction was performed using the "Simultaneous Iterative Reconstruction Technique" (SIRT) with 25 iterations implemented in Inspect3D. Amira (Visage Imaging GmbH) was used for the visualization of the reconstructed volume. An animated version of the tomogram is also provided in the supporting information as video.

A Bruker AMX300 spectrometer (7.0 T) was used to record ^{29}Si MAS NMR spectra of powder samples packed in 4 mm Zirconia rotors spun at a spinning frequency of 6 kHz. The resonance frequency of ^{29}Si at this field is 59.63 MHz. 1000 to 4000 scans were accumulated with a recycle delay of 60 s and a pulse length of 5.0 μs. The chemical shift reference used was tetramethylsilane (TMS). A Bruker Avance DSX400 spectrometer (9.4 T) was used to record the

^{27}Al MAS NMR spectra of spinning (20 kHz) powder samples in 2.5 mm Zirkonia rotors with an ^{27}Al resonance frequency of 104.26 MHz. Data was recorded using single-pulse excitation, accumulating 36000 scans with a recycle delay of 100 ms and pulse length of 0.30 μs. All chemical shifts are reported relative to the reference shift of 0.1 M aqueous solution of $Al(NO_3)_3.9\ H_2O$ (0 ppm).

Cs sorption. Cs sorption experiments were run using ^{137}Cs spiked solutions. ^{137}Cs was purchased from Polatom as carrier-free ^{137}CsCl dissolved in 0.1M HCl. Upon arrival, this solution (0.1 mL; 925 MBq cm^{-3}; 3220 GBq g^{-1}; 2.1x10^{-3} M Cs^+) was diluted 10 times with MQ water in the conical bottom vial in which the spike was delivered. For the sorption experiments, this initial stock solution was further diluted with stable $CsNO_3$ solutions prepared in the respective concrete pore water or mono-ionic electrolyte solution to reach a final ^{137}Cs concentration of 3.1x10^{-12} M.

100 mg of the zeolite, previously equilibrated with YCW, was mixed with 20 mL of its respective ^{137}Cs spiked concrete pore water with varying concentrations of CsCl (10^{-4}, 10^{-5}, 10^{-6}, 5x10^{-7}, 10^{-7} and 10^{-10}) in Oak Ridge centrifuge tubes. These tubes were equilibrated together with their respective blanks (Cs-containing pore water without zeolite) at 25°C on a rotary shaker. After different equilibration times, the samples were centrifuged at 25°C with a cut-off of 85nm (Beckman, J2-HS, JA-17, 20 min, 10000 rpm, 25°C). Upon centrifugation 1ml aliquots of the supernatant phase were transferred to liquid scintillation vials, mixed with 2 ml Ultima Gold XR (Packard) scintillation gel and counted in a Tricarb 2800 (Packard) liquid scintillation counter.

Chabazite standardization and pre-equilibration in YCW. The chabazite powder was sieved over a 50 μm stainless steel Retsch sieve (DIN-ISO: 3310/1) using a pH 8.5 NaOH

177 solution prepared from twice distilled water. The zeolite fraction passing the sieve was then
178 transferred to 250 mL centrifuge cups while adjusting the total volume to 250 mL. In a next step,
179 the suspension was centrifuged with a cut-off of 1 μm (JA-14, 5 min, 2000 rpm) to obtain the
180 zeolite fraction with dimensions between 1 and 50 μm. After centrifugation 200 mL of the
181 supernatant solution was discarded, followed by addition of 200 mL of a 1 N $NaNO_3$ solution
182 titrated to pH 8.5 with NaOH. Following re-suspension of the pellet, the system was equilibrated
183 overnight on an end-over-end shaker and subsequently centrifuged with a cut-off of 1 μm, while
184 discarding the supernatant solution. This washing step was repeated 3 times to obtain a well-
185 defined sodium exchanged zeolite fraction with dimensions between 1 and 50 μm. The resulting
186 Na-form zeolite material was then desalinated by three additional washing steps of 15 minutes;
187 initially with 0.1 N $NaNO_3$ solutions at pH 8 and afterwards twice with ultrapure water (MilliQ)
188 titrated to pH 8 with NaOH. The resulting standardized material was dried at 65°C (96 h) and
189 subsequently stored in an exsiccator over a saturated LiCl solution.
190 During pre-equilibration 2 g of standardized chabazite in its Na-form were washed three times
191 for 24 h at 25°C with 20 mL of the respective concrete pore water. After every washing step the
192 zeolite was separated from the supernatant by centrifugation (Beckman, J2-HS, JA-17, 5min,
193 2000 rpm, 25°C) and 17 ml of the supernatant solution was exchanged with new concrete pore
194 water solution. Following pre-equilibration the zeolite material was washed twice with MilliQ
195 water (15 minutes) to remove the interstitial solutions; centrifuged at 7000rpm for 10 minutes to
196 allow removing the maximum amount of supernatant solution and dried at 65°C (72h). The dried
197 material was stored in an exsiccator over a saturated LiCl solution until further use.
198
199

RESULTS AND DISCUSSION

$^{137}Cs^{+}$ sorption. Cation exchange isotherms recorded as function of time for a highly selective ion like Cs^{+}, provide a sensitive probe for small changes in site selectivity and availability [9, 10], and hence offer a means to assess zeolite stability as function of time. Cs^{+} sorption data for chabazite (Si/Al = 2.1), synthesized using FAU-type zeolite, show constant initial K_D values around 550 l kg^{-1} in YCW electrolyte solution with concentration range of 10^{-10} to 10^{-4} M Cs^{+}. In the timeframe from 1 to 105 days, K_D slightly decreased, but remained higher than 500 l kg^{-1} (Figure 1).

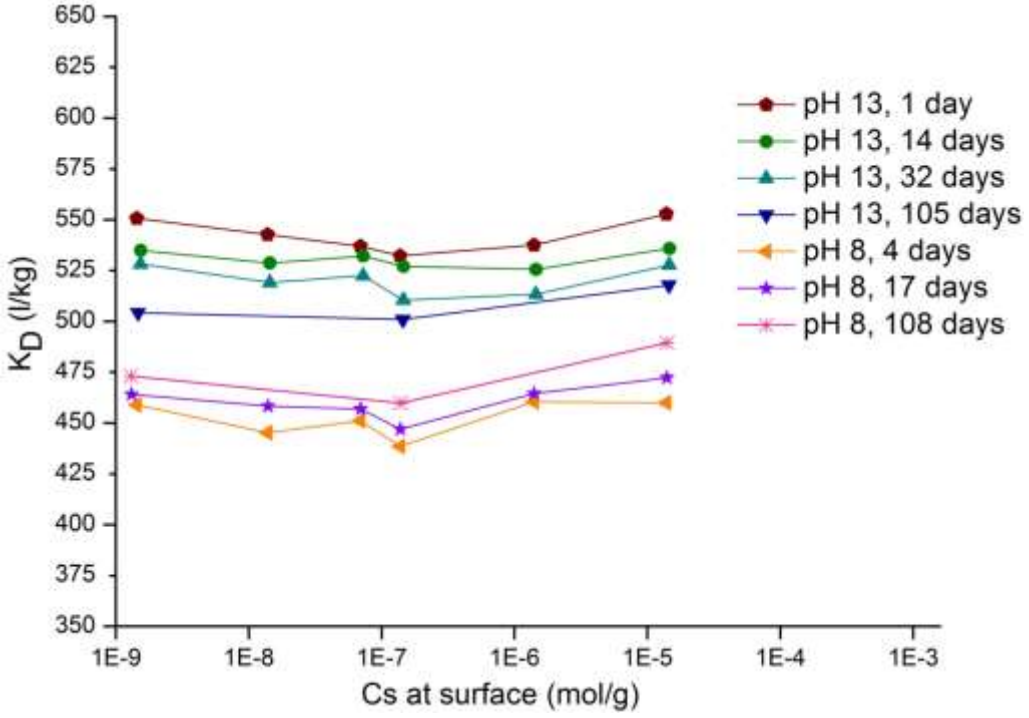

Figure 1. Cs^{+} exchange on chabazite equilibrated with concrete pore water. The standard deviation (1σ) calculated for the reported K_D values are ± 2 l kg^{-1}.

In related electrolyte solutions at pH 8 (See Table SI- 2 for composition), the observed K_D values (460 l kg^{-1}) were significantly lower, showing a slight upward trend with time. Consequently, hydroxyl induced structural alteration is considered as the most likely explanation both for increased K_D with increasing pH, and slight time-dependent decrease of the

hyperalkaline distribution coefficients, which cannot be attributed to slow diffusion of Cs^+ into the zeolite structure. As the high selectivity of chabazite for Cs^+, previously documented in circumneutral conditions,[18] now also has been established in hyper alkaline cementitious environment, evaluation of the framework stability remains the most important prerequisite to enable long-term application in such conditions.

Short-term zeolite stability can be verified by structural characterization of a sample series equilibrated in hyper alkaline media as function of time. A similar evaluation of the long-term stability over decades and centuries is experimentally unfeasible and should be approached differently. Recently, hyper alkaline transformation from zeolite Y (FAU) to various zeolite topologies by exposure to different alkali cations was demonstrated,[28] in analogy to the formation of CHA from FAU in 1 M KOH, originally reported by Bourgogne *et al.*[33] By exposure of FAU type zeolite to hydroxide solution (1 M) at 95°C, phase pure ABW, CHA, MER and ANA frameworks were obtained within 4 days using LiOH, KOH, RbOH and CsOH, respectively. Recrystallization in NaOH occurred much slower, yielding only traces of zeolite P after 4 days. Since YCW essentially is a hyper alkaline solution containing 0.18 M KOH and 0.07 M NaOH, transformation of FAU into CHA is also expected in such media, which would provide a first hint towards chabazite long-term stability in YCW. Subsequent observation of short-term stability and the mechanistic understanding of framework transformations are currently considered as the most feasible and reliable pathway for gaining insight into the long-term stability of CHA in cement derived pore water solutions.

Zeolite Y transformation in YCW. Commercial zeolite Na-Y (Zeocat) was exposed to simulated state I concrete pore water (pH 13), instead of pure 1 M alkali metal hydroxide solution. As the K/Na ratio of the pore water is 2.5/1, chabazite was expected to form, but only

after a longer incubation period due to the lower total hydroxide concentration, resulting in a slower hydrolysis of the zeolite Y framework.[35] The XRD patterns shown in Figure 2 demonstrate that only after 91 days at 85°C the (100) reflection of chabazite appears at 9.52 °2θ.

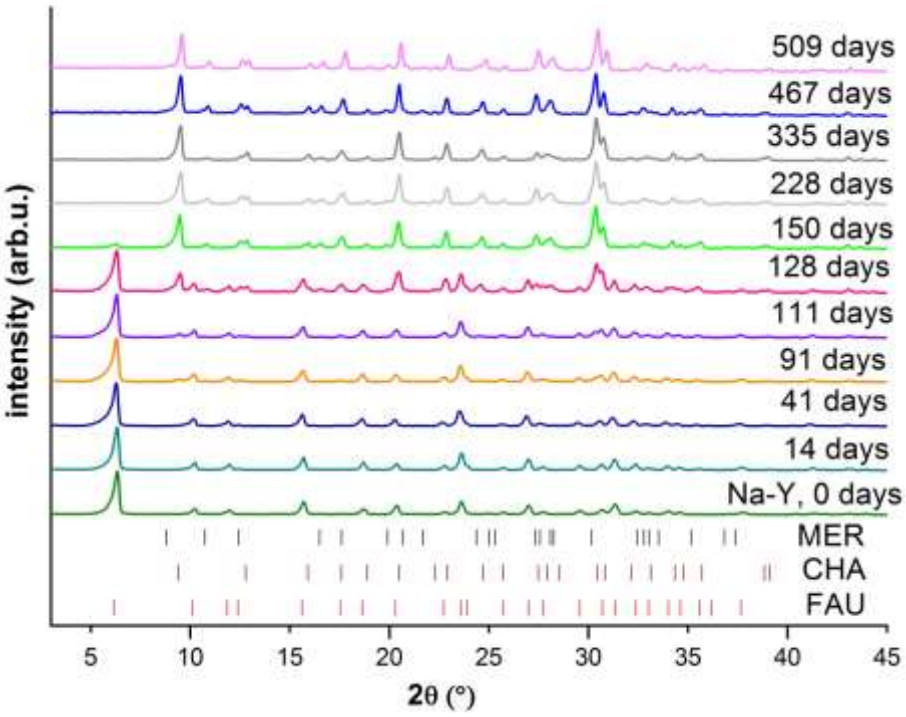

Figure 2. Transformation of zeolite Y in simulated YCW at 85°C under rotation. The presence of CHA type zeolite is detected after 91 days.

This indicates transformation has been initiated between 41 and 91 days. After 150 days, zeolite Y is almost fully transformed. Further XRD patterns of the solid phase products sampled up to 509 days remain similar, indicating that a product, stable in concrete pore water, is obtained. This product is a mixture of chabazite and merlinoite (MER). A MER fraction is already clearly present in the 150 days sample (Figure 2), when FAU is not yet fully transformed, and has not distinctly increased after 509 days. In the series of zeolite Y exposed to concrete pore water at 60°C in static conditions, reflections of chabazite appeared between 224 to 299 days (Figure 3), implying a significant delay of chabazite nucleation at 60°C compared to

85°C. The analysis of the last sample, separated after 837 days, revealed an almost complete transformation of zeolite Y. In Figure 4, the powder XRD patterns of the transformation products of both temperature series are compared, showing that also in the low temperature series a MER type side phase is present next to chabazite. Due to potential differences in water content and chemical composition of these porous samples, the relative amount of both phases is only precisely determined by the Rietveld refinement method.

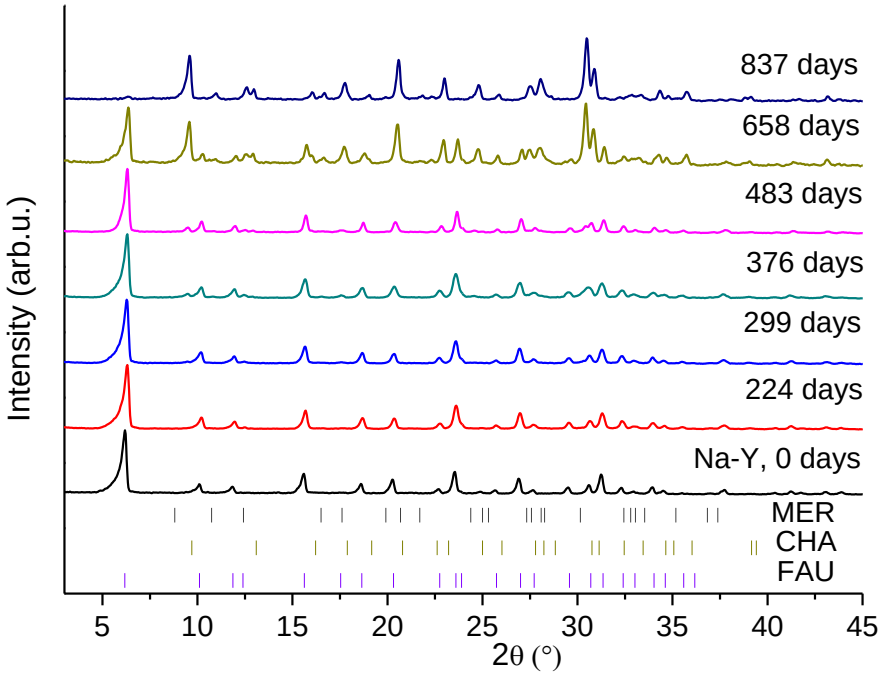

Figure 3. Transformation of zeolite Y in simulated YCW at 60°C (static). CHA is detected after 299 days.

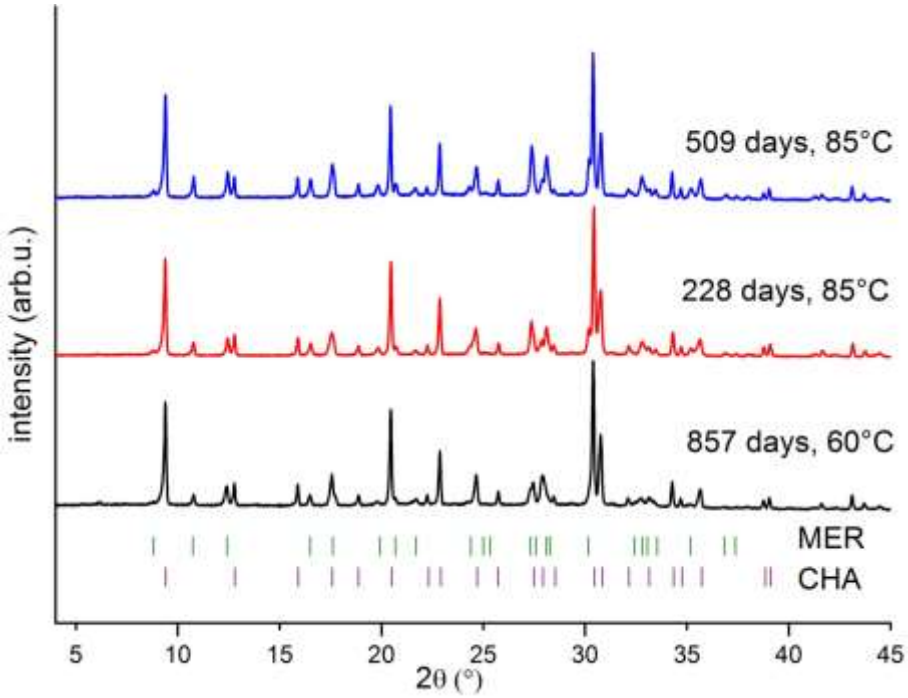

Figure 4. Comparison of the (hydrated) products of the transformation series at 60°C and 85°C.

SEM analysis of the fully transformed products (Figure 5) shows large (up to 50 µm) twinned MER type zeolite rods,[36] which are easily distinguished from the 1-2 micron clustered CHA crystals in the samples. From the SEM images, it is clear that the mixture formed at 60°C contains significantly less MER type crystals relative to CHA (Figure SI 1). At 85°C, no indication for an significant change of the MER/CHA ratio was observed with time.

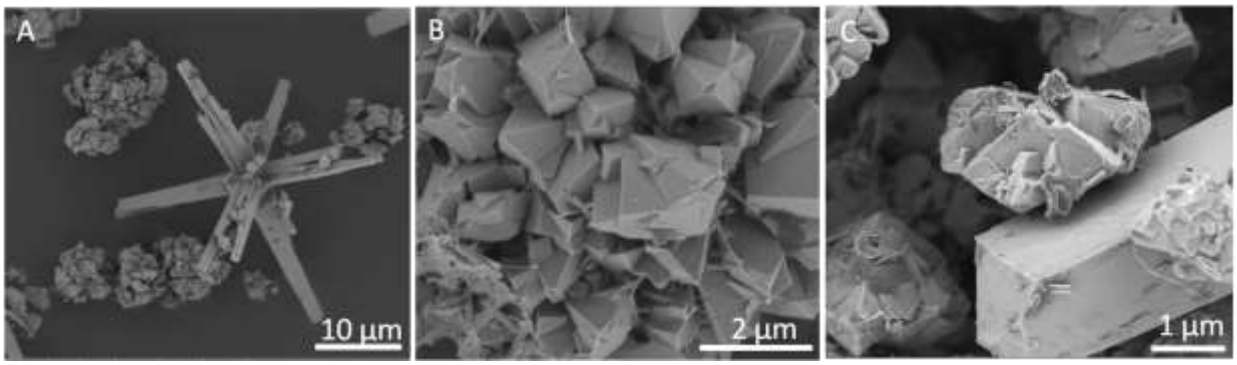

Figure 5. SEM images of the products of the 85°C series: A) MER rods with aggregated CHA crystals (228 days sample) B) Detail of the CHA fraction (228 days sample), C) MER and CHA type crystal (509 days sample).

The appearance of MER in the YCW based transformation was rather unexpected. Although synthetic merlinoite is typically produced by direct synthesis using batch compositions similar to those resulting in chabazite, MER is only obtained by increasing either the temperature, or the K^+ concentration relative to the synthesis composition for CHA synthesis [32, 37] In case of the exposure of FAU to pure KOH, transformation to chabazite was found to occur in a broad range of conditions, and at most trace amounts of MER were encountered, especially at increased temperatures. Once formed in experiments using pure 1 M KOH solutions at 85°C, phase pure chabazite remained stable for more than 2 months, without any appearance of MER. Nevertheless, the occurrence of MER in the transformation of zeolite Y in state I concrete pore water does corroborate results from Fernandez *et al*.,[26] observing MER as the main transformation product in the reaction of FEBEX bentonite with alkaline pore water (pH = 13.5) at 90°C. Using SEM, Fernandez *et al*. demonstrated the growth of MER at the expense of CHA and formulated a hypothesis that a structure directing factor in montmorillonite induced formation of metastable chabazite, which readily transforms to MER.[26] Within the timeframe studied in this work, no clear evidence of chabazite transforming into merlinoite was obtained. However, in the final sample of the series at 85°C, the chabazite crystal surfaces become less smooth and show pitting (Figure 5 C). Combining results reported in literature with the here observed difference observed for FAU conversion in pure KOH versus concrete pore water, it seems obvious MER formation is favoured by slow conversion (lower pH) in systems containing Ca^{2+} (and Mg^{2+} [26]) in combination with K^+.

Zeolite Y transformation in pure KOH. Though conversion of FAU in homo-ionic KOH solutions nowadays is a standard method to synthesize phase pure CHA, full understanding of the mechanism of this transformation is lacking. For elucidation of this mechanism, it is essential to complement the information available from bulk characterization of solid and liquid phases, with techniques providing more local information such as electron or atomic force microscopy.[38, 39] Since the irregular size and morphology of commercially available zeolite Y crystals prevent unambiguous evaluation of the transformation process, well-defined 1 μm octahedral crystals were synthesized with a crown ether template. Upon exposure of this zeolite (Si/Al= 3.5) to KOH solution, liquid phase characterization of the supernatant solutions demonstrated a steadily increasing Si concentration between 0 and 7 hours of equilibration (Figure SI 2). Compared to Si, the Al content in solution not only was significantly lower, its concentration did only increase during first 40 minutes, followed by a steady decrease until at complete phase transformation almost no Al was left in solution.

Only after 22 hours of treatment with KOH at 85°C PXRD showed reflections of CHA in addition to the reflections of the FAU starting material (Figure SI 3).

Electron Microscopy A SEM study of the solid phases during the FAU-CHA transformation process indicated the nucleation of particles commencing initially at the crystal facets of the FAU starting material already after 7 hours (**Figure 6**), which coincides with the stabilization of the Si concentration in the supernatant solution. Fast Fourier transformation (FFT) patterns collected from different regions on high resolution TEM images of the sample showed crystalline order in accordance with sets of lattice planes originating from a single crystalline CHA phase (Figure SI 4), on top of the the still persisting FAU crystals. The similarity in the PXRD peak profiles indicated no significant loss of crystallinity of remaining FAU during the

315 transformation (Figure SI 3). According to the SEM analysis, transformation of FAU into
316 submicron sized CHA crystals was complete in 72 h (**Figure 6**). In addition, it should be noted
317 that the chabazite crystals observed in presence of pure KOH are significantly smaller compared
318 to those obtained in YCW after longer exposure times.

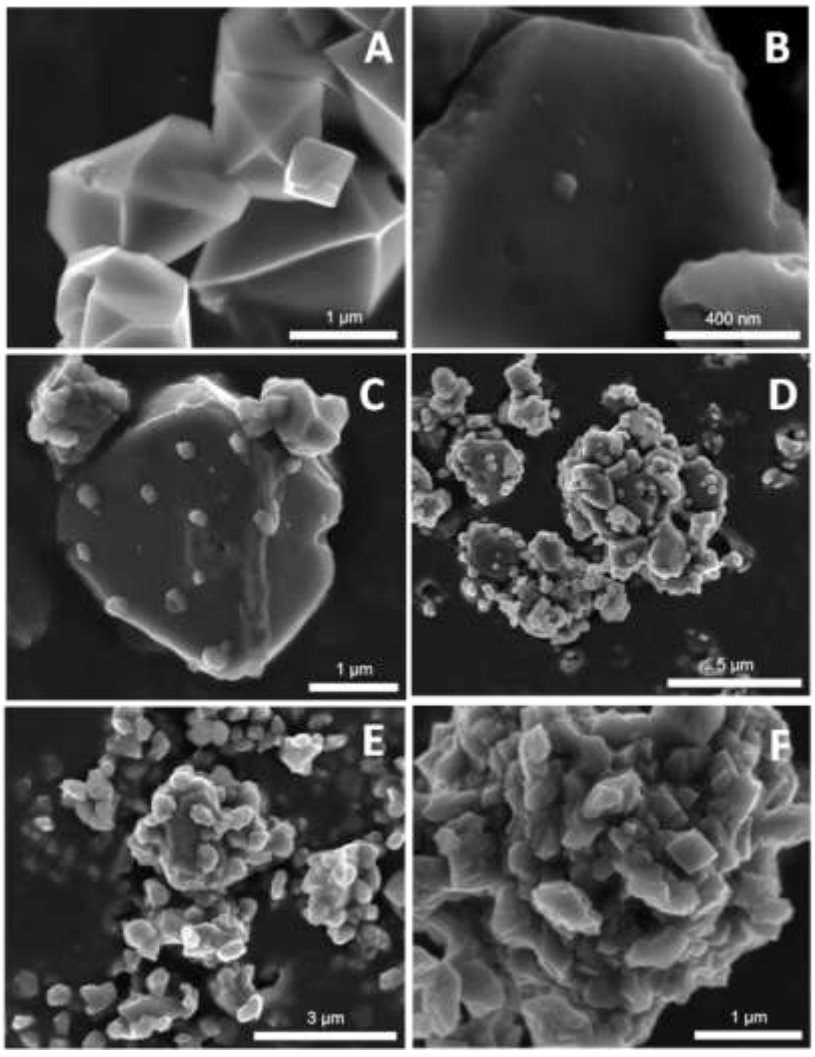

319

320 **Figure 6**. SEM images of the transformation products recorded after 0 h (A), 7 h (B), 22 h (C),
321 36 h (D), 60 h (E) and 72 h (F).

322 Electron tomography results showed that after few hours in hydroxide solution, the zeolite Y
323 crystals were etched (Figure 7). After 22 hours, FAU crystals appeared to have become hollow
324 starting from a single crystal edge, or more commonly, apex of the octahedral crystals. A similar

observation of hollow crystals, previously described for silicalite-1 (MFI), was tentatively explained by the presence of increased concentrations of defect sites at the inside of the crystal where growth was initiated,[40] possibly coupled with an improved crystallinity at the outer surfaces by local Ostwald ripening, or protection of the external surface by interaction with the structure directing cation TPA^{+}.[41] In the current case however, the hollow crystals most probably result from a non random Al distribution in the framework, which is typical for zeolites made with crown-ether templates.[42, 43]

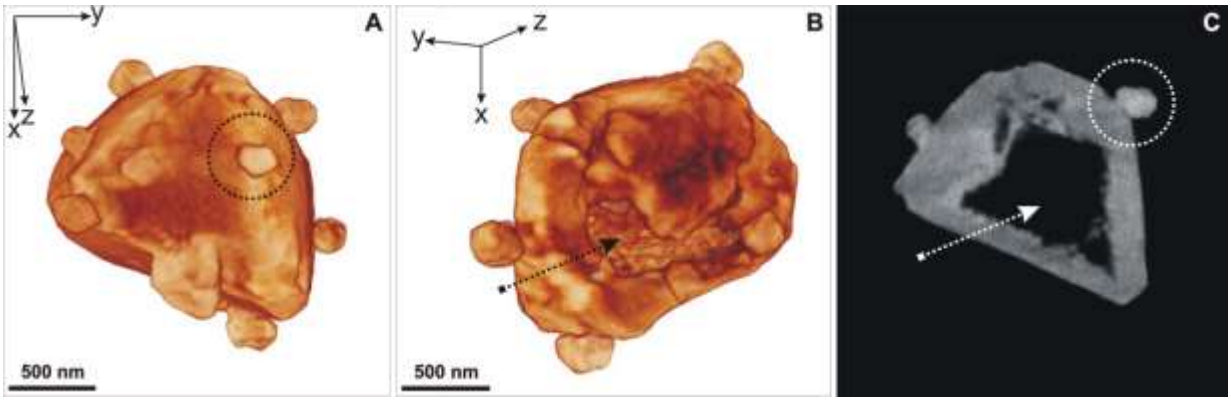

Figure 7. Visualizations of the 3D tomographic reconstruction from a FAU crystal depicted along different orientations are given in (A) and (B). A slice through the 3D reconstruction is presented in (C), in which both the hollow structure of the crystal and newly formed CHA crystal are indicated.

^{29}Si MAS NMR determined Si/Al ratios in the solid phase show a decrease from 3.5 in the FAU starting material to 2.0 at the onset of CHA formation (Table SI- 3). At that time, NaY is virtually fully exchanged into the potassium form (K/Na ≥ 40). ^{27}Al MAS NMR of subsamples taken as function of time, demonstrated a preservation of the tetrahedral Al-coordination during the transformation process. The Si/Al ratio of phase pure chabazite obtained after 72 hours is 1.66, and is unchanged after 8 days.

As mentioned earlier, chabazite is formed over a broad range of conditions in presence of K^+. For example, the liquid/solid ratio of 60 used in the experiment described above, can be varied between 9 and 120, still yielding full conversion of FAU to chabazite. Moreover, lower total hydroxide concentrations and mixed K, Na environments enabled chabazite formation too, thereby corroborating the observed CHA formation obtained in YCW. While the combination of FAU transformation experiments in pure hydroxide and simulated YCW solutions provides significant indications for consistent formation of CHA, confirming the long-term stability of CHA in YCW, the crystallization of a significant fraction of MER observed during the transformation in YCW media at temperatures as low as 60°C, was unexpected. It must however be noted that concrete pore water also contains small amounts of Ca^{2+} cations, in addition to K^+ and Na^+. While Ca^{2+} has been demonstrated to exert a stabilizing effect on the FAU structure,[44-46] as confirmed by the absence of chabazite formation upon exposure of Ca-exchanged zeolite Y to KOH (Figure SI 5), it may now be speculated to also influence the ratio of MER/CHA upon hyperalkaline transformation in K^+, Na^+ media. However, for now it remains unclear which parameter facilitated the formation of merlinoite next to chabazite in pore water environment. Future research should focus on the influence of Na/K/Ca ratio, OH^- content, and temperature on the ratio of CHA/MER in the final transformation products, as well as in the silica speciation in presence of these cations. Since it is clear that the formation conditions of these two zeolites are close, it will be extremely difficult to exclude long-term interconversion between these phases. As result, safety assessment of any long-term application of zeolites as sorption sink in hyper-alkaline media will require to document the sorption properties of both phases, to allow construction of a conservative performance assessment scenario. Also the hydroxyl induced changes to the frameworks pointed out by ^{137}Cs, should be elucidated.

366 ASSOCIATED CONTENT

367 **Supporting Information**.

368 Typical porewater compositions for state I porwaters. Evolution of the Cs^+ sorption isotherm as
369 function of time and pH. Spectroscopic and analytical data recorded during the transformation
370 process from FAU to CHA. Animated version of the 3D tomographic reconstruction from a
371 hollow FAU crystal with newly formed CHA crystals on the crystal faces. This material is
372 available free of charge via the Internet at http://pubs.acs.org.

373 **Toc Art**

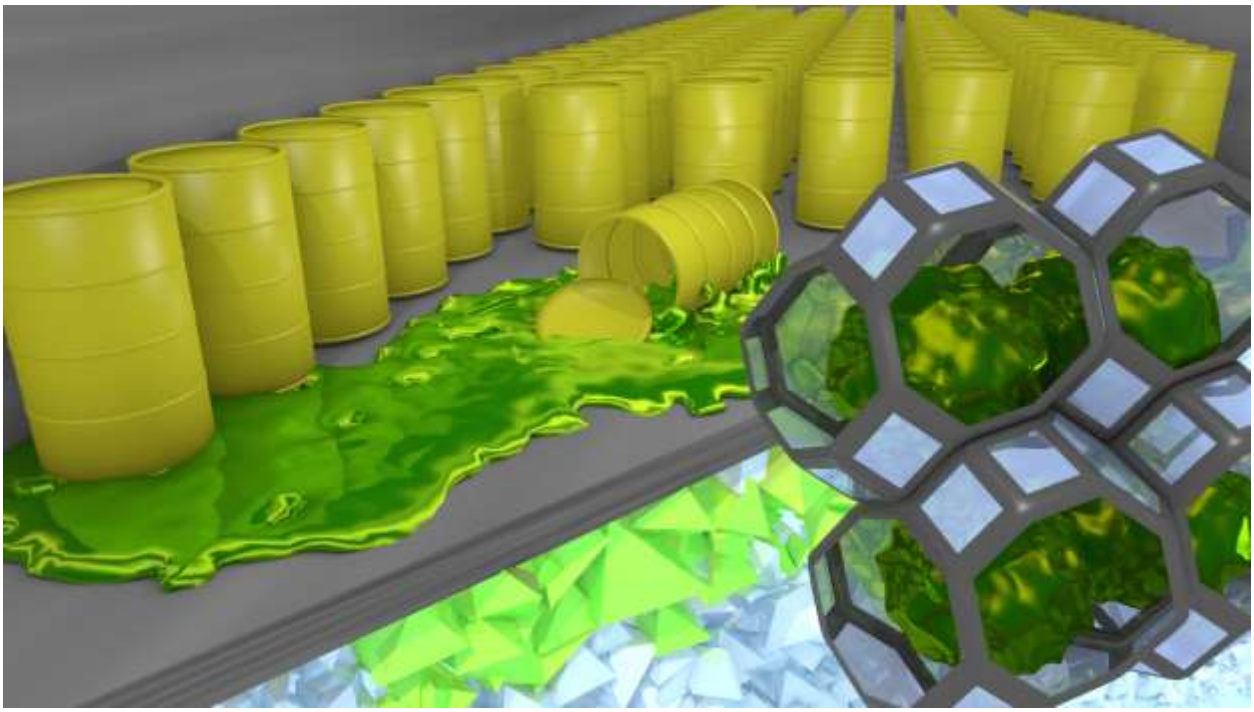

374

375 AUTHOR INFORMATION

376 **Corresponding Author**

377 *eric.breynaert@biw.kuleuven.be. KULeuven – Center for surface chemistry and catalysis.
378 Kasteelpark arenberg 23 – box 2461. B-3001 Leuven. Tel: +32 16 32 1598 Fax: +32 16 32 1998.

Author Contributions

The manuscript was written through contributions of all authors. All authors have given approval to the final version of the manuscript.

Funding Sources

This work was supported by long-term structural funding by the Flemish Government (Methusalem) and by ONDRAF/NIRAS, the Belgian Agency for Radioactive Waste and Fissile Materials, as part of the program on surface disposal of Belgian Category A waste. The Belgian government is acknowledged for financing the interuniversity poles of attraction (IAP-PAI). G.V.T. and S.B. acknowledge financial support from European Research Council (ERC Advanced Grant # 24691-COUNTATOMS, ERC Starting Grant #335078-COLOURATOMS).

ACKNOWLEDGMENT

L. Van Tendeloo and E. Breynaert acknowledge a mandate as, respectively, an aspirant and a postdoctoral fellow of FWO Vlaanderen. This work was partially performed in cooperation with ONDRAF/NIRAS.

REFERENCES

1. Nemerow, N. L.; Agardy, F. J., *Strategies of industrial and hazardous waste management*. Van Nostrand Reinhold: New York, 1998; p 748.
2. Williams, P. T., *Waste treatment and disposal*. 2nd ed.; Wiley: Chichester, West Sussex, England ; Hoboken, NJ, USA, 2005; p 380.
3. Sumerling, T. *Project near surface disposal of category A waste at Dessel*; NIROND-TR 2007-06 E December; Ondraf/Niras: Brussels, 2006; p 90.
4. Niras/Ondraf *The cAt project in Dessel: A long-term solution for Belgian category A waste*; NIROND 2010- 02 E March; Brussels, 2010; p 140.
5. Atkins, M.; Glasser, F. P., Application of portland cement-based materials to radioactive waste immobilization. *Waste Manage. (Oxford)* **1992,** *12*, 105-131.
6. Kim, D.; Quinlan, M.; Yen, T. F., Encapsulation of lead from hazardous CRT glass wastes using biopolymer cross-linked concrete systems. *Waste Manage. (Oxford)* **2009,** *29*, (1), 321-328.

7. Berner, U. R., Evolution of pore water chemistry during degradation of cement in a radioactive waste repository environment. *Waste Manage. (Oxford)* **1992,** *12*, (2-3), 201-219.
8. Jacques, D.; Wang, L.; Martens, E.; Mallants, D., Modelling chemical degradation of concrete during leaching with rain and soil water types. *Cem. Concr. Res.* **2010,** *40*, (8), 1306-1313.
9. Maes, A.; Cremers, A., Site group interaction effects in zeolite-Y. Part 2.-Na-Ag selectivity in different site groups. *Journal of the Chemical Society, Faraday Transactions 1: Physical Chemistry in Condensed Phases* **1978,** *74*, (0), 136-145.
10. Sawhney, B. L., Potassium and cesium ion selectivity in relation to clay mineral structure. *Clays Clay Miner.* **1970,** *18*, 47-52.
11. Pohl, C. A.; Stillian, J. R.; Jackson, P. E., Factors controlling ion-exchange selectivity in suppressed ion chromatography. *J. Chromatogr. A* **1997,** *789*, (1-2), 29-41.
12. Fritz, J. S., Factors affecting selectivity in ion chromatography. *J. Chromatogr. A* **2005,** *1085*, (1), 8-17.
13. Mimura, H.; Akiba, K., Adsorption Behavior of Cesium and Strontium on Synthetic Zeolite P. *J. Nucl. Sci. Technol.* **1993,** *30*, (5), 436-443.
14. Samanta, S. K., Cesium sorption behavior of a mordenite type synthetic zeolite and its modified form obtained by acid treatment. *J. Radioanal. Nucl. Chem.* **1999,** *240*, (2), 585-588.
15. Mimura, H.; Kanno, T., Distribution and Fixation of Cesium and Strontium in Zeolite A and Chabazite. *J. Nucl. Sci. Technol.* **1985,** *22*, (4), 284-291.
16. Ames, L. L. J., Effect of base cation on the cesium kinetics of clinoptilolite. *The American Mineralogist* **1962,** *47*, 1310-1316.
17. Hoyle, S.; Grutzeck, M. W., Effects of Phase Composition on the Cesium Leachability of Cement-Based Waste Forms. In *Waste management '86: waste isolation in the U.S., technical programs and public education : proceedings of the Symposium on Waste Management at Tucson, Arizona, March 2-26 1986*, Arizona Board of Regents: 1986; pp 491-496.
18. Borai, E. H.; Harjula, R.; Malinen, L.; Paajanen, A., Efficient removal of cesium from low-level radioactive liquid waste using natural and impregnated zeolite minerals. *J. Hazard. Mater.* **2009,** *172*, (1), 416-22.
19. Hsu Liu, D. C. C. H. P. C. N., Evaluation of cesium sorption on natural mordenite. *J. Radioanal. Nucl. Chem.* **1994,** *185*, 319-329.
20. Abusafa, A.; Yücel, H., Removal of 137Cs from aqueous solutions using different cationic forms of a natural zeolite: clinoptilolite. *Sep. Purif. Technol.* **2002,** *28*, (2), 103-116.
21. Mimura, H.; Yamagishi, I.; Akiba, K., Removal of Cesium and Strontium from High-Activity-Level water by zeolites. *Bulletin of the Research Institute of Mineral Dressing and Metallurgy* **1988,** *44*, (1), 1-7.
22. Chang, H.-s.; Um, W.; Rod, K.; Serne, R. J.; Thompson, A.; Perdrial, N.; Steefel, C. I.; Chorover, J., Strontium and Cesium Release Mechanisms during Unsaturated Flow through Waste-Weathered Hanford Sediments. *Environ. Sci. Technol.* **2011,** *45*, (19), 8313-8320.
23. Faghihian, H.; Ghannadi Marageh, M.; Kazemian, H., The use of clinoptilolite and its sodium form for removal of radioactive cesium, and strontium from nuclear wastewater and Pb2+, Ni2+, Cd2+, Ba2+ from municipal wastewater. *Appl. Radiat. Isot.* **1999,** *50*, (4), 655-660.
24. Bostick, D. T.; Arnold Jr., W. D.; Taylor, P. A.; McTaggart, D. R.; Burgess, M. W.; Guo, B. In *Evaluation of Improved Techniques for the Removal of 90Sr and 137Cs from Process Wastewater and Groundwater: Chabazite Zeolite Baseline Study*, Energy, 1995; 1995; p 35.

25. Misaelides, P., Application of natural zeolites in environmental remediation: A short review. *Microporous Mesoporous Mater.* **2011,** *144*, 15-18.
26. Fernández, R.; Rodríguez, M.; Vigil De La Villa, R.; Cuevas, J., Geochemical constraints on the stability of zeolites and C–S–H in the high pH reaction of bentonite. *Geochim. Cosmochim. Acta* **2010,** *74*, (3), 890-906.
27. Wallace, S. H.; Shaw, S.; Morris, K.; Small, J. S.; Burke, I. T., Alteration of sediments by hyperalkaline K-rich cement leachate: implications for strontium adsorption and incorporation. *Environ. Sci. Technol.* **2013,** *47*, 3694-700.
28. Van Tendeloo, L.; Gobechiya, E.; Breynaert, E.; Martens, J. A.; Kirschhock, C. E. A., Alkaline cations directing the transformation of FAU zeolites into five different framework types. *Chem. Commun.* **2013**, 1-3.
29. Honda, K.; Itakura, M.; Matsuura, Y.; Onda, A.; Ide, Y.; Sadakane, M.; Sano, T., Role of structural similarity between starting zeolite and product zeolite in the interzeolite conversion process. *Journal of nanoscience and nanotechnology* **2013,** *13*, (4), 3020-6.
30. Sano, T.; Itakura, M.; Sadakane, M., High Potential of Interzeolite Conversion Method for Zeolite Synthesis. *Journal of the Japan Petroleum Institute* **2013,** *56*, 183-197.
31. Feijen, E. J. P.; De Vadder, K.; Bosschaerts, M. H.; Lievens, J. L.; Martens, J. A.; Grobet, P. J.; Jacobs, P. A., Role of 18-Crown-6 and 15-Crown-5 Ethers in the Crystallization of Polytype Faujasite Zeolites. *J. Am. Chem. Soc.* **1994,** *116*, 2950-2957.
32. Robson, H. E., *Verified syntheses of zeolitic materials*. Elsevier: 2001; p 272.
33. Bourgogne, M.; Guth, J. L.; Wey, R. Process for the preparation of synthetic zeolites, and zeolites obtained by said process. 4 503 024, 1985.
34. Parkhurst, D. L.; Appelo, C. A. J. *User's guide to PHREEQC (Version 2) : a computer program for speciation, batch-reaction, one-dimensional transport, and inverse geochemical calculations*; Denver, Colorado, 1999.
35. Cizmek, A.; Subotic, B.; Aiello, R.; Crea, F.; Tuoto, C., Dissolution of high-silica zeolites in alkaline solutions I. Dissolution of silicalite-1 and ZSM-5 with different aluminum content. *Microporous Mater.* **1995,** *4*, 159-168.
36. Haouas, M.; Lakiss, L.; Martineau, C.; El Fallah, J.; Valtchev, V.; Taulelle, F., Silicate ionic liquid synthesis of zeolite merlinoite: Crystal size control from crystalline nanoaggregates to micron-sized single-crystals. *Microporous Mesoporous Mater.* **2014,** *198*, (0), 35-44.
37. Skofteland, B. M.; Ellestad, O. H.; Lillerud, K. P., Potassium merlinoite: crystallization, structural and thermal properties. *Microporous Mesoporous Mater.* **2001,** *43*, (1), 61-71.
38. Li, P.; Ding, T.; Liu, L.; Xiong, G., Investigation on phase transformation mechanism of zeolite NaY under alkaline hydrothermal conditions. *Mater. Charact.* **2013,** *86*, 221-231.
39. Wang, Y.; Li, X.; Xue, Z.; Dai, L.; Xie, S.; Li, Q., Preparation of zeolite ANA crystal from zeolite Y by in situ solid phase iso-structure transformation. *J. Phys. Chem. B* **2010,** *114*, (17), 5747-54.
40. Wang, Y.; Tuel, A., Nanoporous zeolite single crystals: ZSM-5 nanoboxes with uniform intracrystalline hollow structures. *Microporous Mesoporous Mater.* **2008,** *113*, (1–3), 286-295.
41. Dai, C.; Zhang, A.; Li, L.; Hou, K.; Ding, F.; Li, J.; Mu, D.; Song, C.; Liu, M.; Guo, X., Synthesis of Hollow Nanocubes and Macroporous Monoliths of Silicalite-1 by Alkaline Treatment. *Chem. Mater.* **2013,** *25*, (21), 4197-4205.
42. Feijen, E. J. P.; Lievens, J. L.; Martens, J. a.; Grobet, P. J.; Jacobs, P. a., Silicon and Aluminum Ordering in Frameworks of FAU and EMT Aluminosilicate Zeolites Crystallized in the Presence of Crown Ethers. *The Journal of Physical Chemistry* **1996,** *100*, 4970-4975.

43. Groen, J. C.; Bach, T.; Ziese, U.; Paulaime-van Donk, A. M.; de Jong, K. P.; Moulijn, J. A.; Pérez-Ramírez, J., Creation of Hollow Zeolite Architectures by Controlled Desilication of Al-Zoned ZSM-5 Crystals. *J. Am. Chem. Soc.* **2005,** *127*, (31), 10792-10793.
44. Chiyoda, O.; Davis, M. E., Hydrothermal conversion of Y-zeolite using alkaline-earth cations. *Microporous Mesoporous Mater.* **1999,** *32*, (3), 257-264.
45. Singh, R.; Dutta, P. K., Stabilization of natural Faujasite zeolite: possible role of alkaline earth metal ions. *Microporous Mesoporous Mater.* **1998,** *21*, (1-3), 103-109.
46. Denayer, J. F. M.; Depla, A.; Vermandel, W.; Gemoets, F.; van Buren, F.; Martens, J.; Kirschhock, C.; Baron, G. V.; Jacobs, P. A., Removal of cyclopentadiene from 1-octene by transition metal containing zeolites-Part 2: Stabilization of CoCaX zeolite by its cation distribution. *Microporous Mesoporous Mater.* **2007,** *103*, (1-3), 11-19.

Supporting Information - Chabazite: Stable cation-exchanger in hyper alkaline concrete pore water

Leen Van Tendeloo,[1] Wauter Wangermez, [1] Mert Kurttepeli, [2] Benny de Blochouse, [1] Sara Bals, [2] Gustaaf Van Tendeloo, [2] Johan A. Martens, [1] André Maes, [1] Christine E.A. Kirschhock, [1] Eric Breynaert[1,].*

[1]Centre for Surface Chemistry and Catalysis, KU Leuven, Kasteelpark Arenberg 23, 3001 Heverlee.

[2]Electron Microscopy for Materials Science (EMAT), University of Antwerp, Groenenborgerlaan 171, 2020 Antwerp;

Table SI- 1: Typical pore water composition (state I, pH 13, 25°C) calculated using PhreeqC with the Lawrence Livermore National Laboratory database llnl.dat.

	Speciation	Molality		Speciation	Molality		Speciation	Molality
Ca		$1{,}5\times10^{-3}$	K		$1{,}8\times10^{-1}$	Na		$7{,}02\times10^{-2}$
	Ca^{2+}	$7{,}08\times10^{-4}$		K^{+}	$1{,}72\times10^{-1}$		Na^{+}	$6{,}87\times10^{-2}$
				KSO_4^{-}	$2{,}52\times10^{-4}$		$NaSO_4^{-}$	$8{,}55\times10^{-5}$
	$CaSO_4$	$6{,}14\times10^{-6}$		KOH	$7{,}31\times10^{-3}$		$NaHCO_3$	$1{,}98\times10^{-9}$
	$CaHCO_3^{+}$	$1{,}03\times10^{-10}$		$KHSO_4$	$8{,}98\times10^{-18}$		$NaCO_3^{-}$	$5{,}33\times10^{-6}$
	$CaCO_3$	$1{,}15\times10^{-5}$					NaOH	$1{,}45\times10^{-3}$
	$CaOH^{+}$	$7{,}74\times10^{-4}$						

Table SI- 2: Typical pore water composition (state I, pH 8, 25°C) calculated using PhreeqC with the Lawrence Livermore National Laboratory database llnl.dat.

	Speciation	Molality		Speciation	Molality		Speciation	Molality

Ca		$1,5x10^{-3}$	K		$1,8x10^{-1}$	Na		$7,01x10^{-2}$
	Ca^{2+}	$1,08x10^{-3}$		K^{+}	$1,8x10^{-1}$		Na^{+}	$7,00x10^{-2}$
	$CaNO_3^{+}$	$4,07x10^{-4}$		KSO_4^{-}	$2,57x10^{-4}$		$NaSO_4^{-}$	$8,51x10^{-5}$
	$CaSO_4$	$9,07x10^{-6}$		KOH	$3,12x10^{-8}$		$NaHCO_3$	$4,73x10^{-6}$
	$CaHCO_3^{+}$	$3,67x10^{-7}$		$KHSO_4$	$2,22x10^{-12}$		$NaCO_3^{-}$	$5,24x10^{-8}$
	$CaCO_3$	$1,67x10^{-7}$					NaOH	$6,06x10^{-9}$
	$CaOH^{+}$	$4,83x10^{-9}$						

525 **Table SI- 3:** Si distribution and Si/Al ratio of the samples during transformation of zeolite Y
526 (Si/Al = 3.5) determined by ^{29}Si MAS NMR.

	$Q^{0\,Al}$(%)	$Q^{1\,Al}$(%)	$Q^{2\,Al}$(%)	$Q^{3\,Al}$(%)	$Q^{4\,Al}$(%)	Si/Al
Na-Y (calc) 0h	16.39	54.84	25.70	3.08	0	**3.46**
FAU 22 h	2.47	27.37	42.90	19.96	7.30	**1.97**
CHA 72 h	3.63	14.61	33.64	33.56	14.55	**1.66**
CHA 8 days	2.77	13.62	32.96	33.96	16.69	**1.61**

527

528

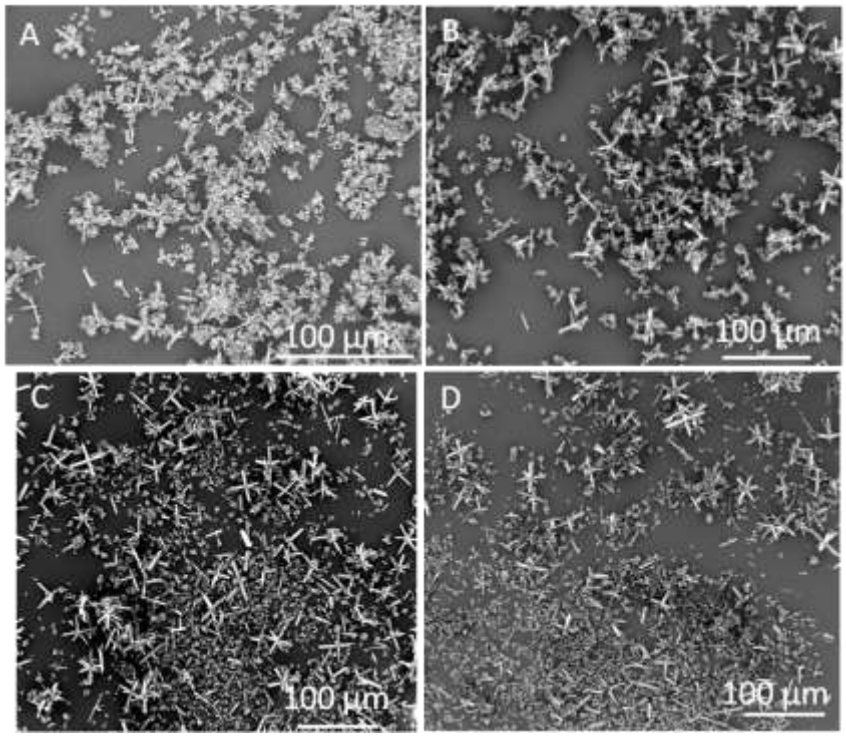

Figure SI 1: SEM images of transformation products after 0 hours (A), 7 hours (B) and 72 hours (C) are presented above. The fast-fourier transforms from the corresponding areas indicated at (B) unveil the CHA content of the newly formed particles.The transformation product formed at 60°C in 857 days (A) contains more chabazite relative to merlinoite than the products at 85°C after 150 days (B), 228 days (C) and 509 days (C).

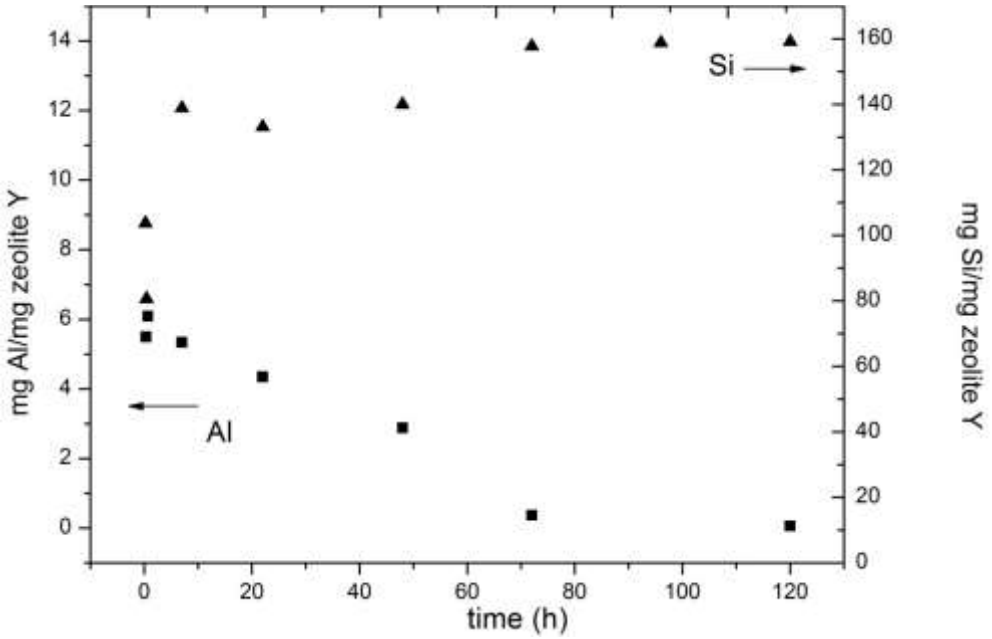

536
537
538 **Figure SI 2:** Concentrations of Al (■) and Si (▲) in the liquid phase during the transformation

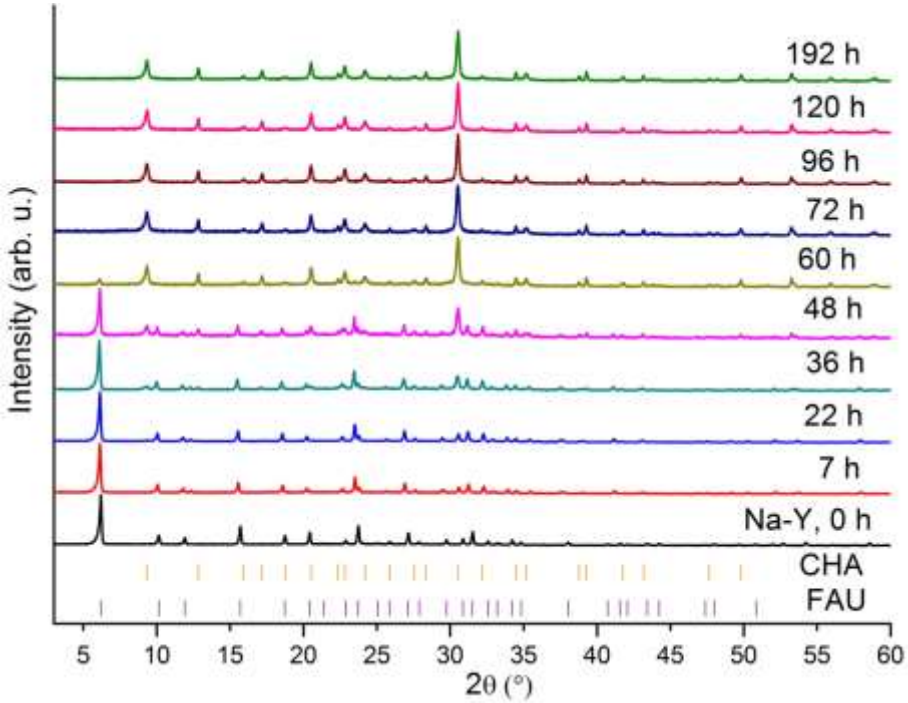

539
540 **Figure SI 3.** Time series of transformation of zeolite Y (Si/Al=3.5) into chabazite in pure KOH
541 as monitored by PXRD. The transformation occurs within 72 hours.

542

543

544

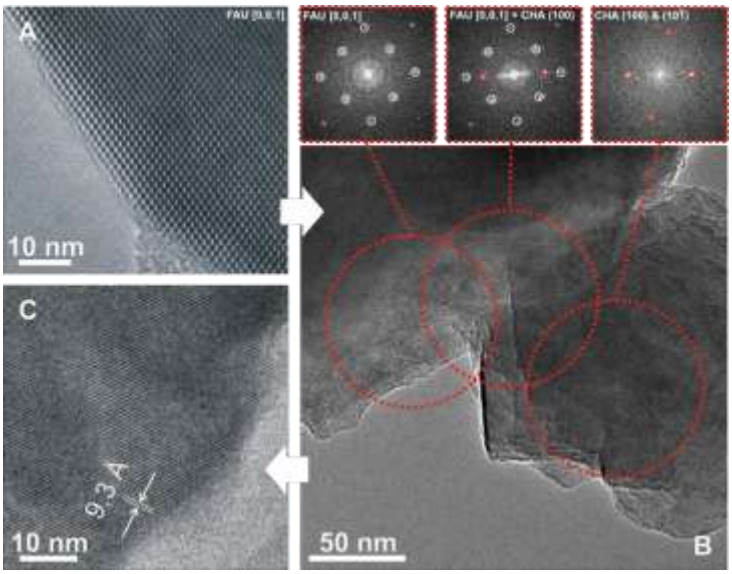

Figure SI 4: High-resolution TEM images of transformation products after 0 hours (A), 7 hours (B) and 72 hours (C) are presented above. The fast-fourier transforms from the corresponding areas indicated at (B) unveil the CHA content of the newly formed particles.

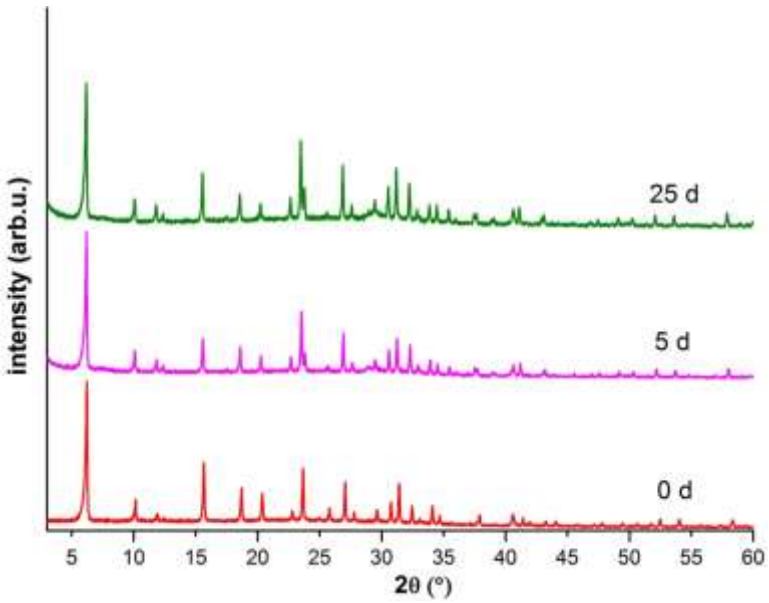

Figure SI 5. Ca-Y (dried at 60°C, non-calcined) does not transform to chabazite within 25 days, whereas under the applied conditions, Na-Y is fully converted into chabazite in 96 hours.